Semi-empirical dissipation source functions for wind-wave models: part I, definition, calibration and validation at global scales.

FABRICE ARDHUIN, RUDY MAGNE, JEAN-FRANÇOIS FILIPOT[1], ANDRE VAN DER WESTHUYSEN[2], AARON ROLAND[3], PIERRE QUEFFEULOU[4], JEAN-MICHEL LEFEVRE, LOTFI AOUF[5], ALEXANDER BABANIN[6], AND FABRICE COLLARD[7]

[1]*Service Hydrographique et Océanographique de la Marine, Brest, France*
[2]*Delft Hydraulics*
[3]*Technological University of Darmstadt, Germany*
[4]*Ifremer, DOPS/LOS*
[5]*UMR GAME, Météo-France - CNRS, Toulouse, France*
[6]*Swinburne University, Hawthorn, VA, Australia*
[7]*CLS, Division Radar, Plouzané, France*

(Manuscript received , in final form)

ABSTRACT

Based on observations, new parameterizations for the spectral evolution of wind-generated waves due to wave breaking and swell dissipation are proposed. The proposed rates of dissipation have no predetermined spectral shapes and are functions of the wave spectrum and wind speed and direction, in a way consistent with observation of wave breaking and swell dissipation properties. Namely, the swell dissipation in nonlinear and proportional to the swell slope, and dissipation due to wave breaking only occur when the non-dimensional spectrum exceeds the observed threshold. At high frequency, an additional source of short wave dissipation due to long wave breaking is needed. Several degrees of freedom are introduced in the wave breaking formulation, together with an adjustment of the wind-wave generation term of Janssen (J. Phys. Oceanogr. 1991), in order to be able to reproduce observed spectral shapes and the variability of several spectral moments with wind speed and wave height. These parameterizations are first combined and calibrated with the Discrete Interaction Approximation of Hasselmann et al. (J. Phys. Oceangr. 1985) for the nonlinear interactions. The wind-wave energy balance is verified in a wide range of conditions and scales in order to demonstrate the robustness of the parameterizations, from gentle swells to category 5 Hurricanes, from the global ocean to coastal settings and small lakes. Likewise, wave height, peak and mean periods, and spectral data are validated using in situ and remote sensing data. Although some systematic defects are still present, the parameterizations yield the best overall results to date, especially for significant wave heights, directions and mean periods. Two source term settings are proposed, one that gives the best fit for average sea states and parameters related to the high frequency waves, and another that provides the best fit for very large sea state, for which the relative errors are actually smallest. The implementation in four wave models, WAVEWATCH III, WAM, WWM and SWAN shows that, on average, when reasonably numerical schemes are used, the result quality in terms of H_s, T_p and T_{m02} is mostly a function of the quality of the wind forcing and of the parameterizations of physical processes.

1. Introduction

Spectral wave modelling has been performed for the last 50 years, using the wave energy balance equation (Gelci et al. 1957). This description radiation of the spectral density of the surface elevation variance F distributed over frequencies f and directions θ can be put in the form

$$\frac{\mathrm{d}F(f,\theta)}{\mathrm{d}t} = S_{\mathrm{atm}}(f,\theta)+S_{\mathrm{nl}}(f,\theta)+S_{\mathrm{oc}}(f,\theta)+S_{\mathrm{bt}}(f,\theta), \quad (1)$$

where the Lagrangian derivative is the rate of change of the spectral density when following a wave packet at its group speed in physical and spectral space. The source functions on the right hand side are separated into an atmospheric source function S_{atm}, a nonlinear scattering term S_{nl}, an ocean source S_{oc}, and a bottom source S_{bt}.

Corresponding author address: Fabrice Ardhuin, Service Hydrographique et Océanographique de la Marine, 29609 Brest, France
E-mail: ardhuin@shom.fr

This separation is somewhat arbitrary, but, compared to the usual separation of deep-water evolution in input, non-linear interactions, and dissipation, it has the benefit of identifying where the energy and momentum is going to or coming from.

$S_{\rm atm}$, which gives the flux of energy from the atmospheric non-wave motion to the wave motion, is the sum of a wave generation term $S_{\rm in}$ and a wind-generation term $S_{\rm out}$ (often referred to as negative wind input, i.e. a wind output). The nonlinear scattering term $S_{\rm nl}$ represents all processes that lead to an exchange of wave energy between the different spectral components. In deep and intermediate water depth, this is dominated by cubic interactions between quadruplets of wave trains, while quadratic nonlinearities play an important role in shallow water (WISE Group 2007). The ocean source $S_{\rm oc}$ may accomodate wave-current interactions[1] and interactions of surface and internal waves, but it will be here restricted to wave breaking and wave-turbulence interactions.

The basic principle underlying that equation is that waves essentially propagate as a superposition of almost linear wave groups that evolve on longer time scales as a result of weak-in-the-mean processes (e.g. Komen et al. 1994). Recent review have questioned the possibility of further improving numerical wave models without changing this basic principle (Cavaleri 2006). Although this may be true in the long term, we demonstrate here that it is possible to improve model results significantly by including more physical constraints in the source term parameterizations. The main advance proposed in the present paper is the adjustment of a shape-free dissipation function based on today's knowledge on the breaking of random waves (Banner et al. 2000; Babanin et al. 2001) and the dissipation of swells over long distances (Ardhuin et al. 2009b). Although the present formulations are still semi-empirical, in the sense that they are not based on a detailed physical model of dissipation processes, they demonstrate that progress is possible. This effort opens the way for completely physical parameterizations (Filipot et al. 2008) that will eventually provide new applications for wave models, such as the estimation of whitecap coverage and foam thickness.

Essentially, all wave dissipation parameterizations up to the work of (van der Westhuysen et al. 2007) had no quantitative relationship with observed features of wave dissipation, and the parameterizations were generally used as a tuning knob to close the wave energy balance. A preliminary attempt by (Alves and Banner 2003) tried to incorporate some observed aspects of wave breaking revealed by (Banner et al. 2000), but this was not quantitatively correct (Babanin and van der Westhuysen 2008), and was further combined with the dissipation function of the kind given (Komen et al. 1984), which has nothing to do with observations and produces some very unrealistic results.

The parameterization of the form proposed by Komen et al. (1984) have produced a family loosely justified by the so-called "random pulse" theory of (Hasselmann 1974). These take a generic form

$$S_{\rm oc}\left(f,\theta\right) = C_{\rm ds} g^{0.5} k_x^{4.5} H_s^4 \left[\delta_1 \frac{k}{k_x} + \delta_2 \left(\frac{k}{k_x}\right)^2\right], \tag{2}$$

in which $C_{\rm ds}$ is a negative constant, and k_x is an energy-weighted mean wavenumber defined from the entire spectrum, and H_s is the significant wave height. In the early and latest parameterizations, the following definition was used

$$k_x = \left[\frac{16}{H_s^2}\int_0^{f_{\max}}\int_0^{2\pi} k^p E\left(f,\theta\right) {\rm d}f{\rm d}\theta\right]^{1/p}, \tag{3}$$

where p is a chosen constant, typically $p = 0.5$.

These parameterizations are still widely used and in spite the fact that the underlying theory is not self-consistent: indeed, if whitecaps do act as random pressure pulses their average work on the underlying waves only occurs because of a phase correlation between the vertical orbital velocity field and the moving whitecap position, so that not all wave components are dissipated by a given whitecap and the dissipation function cannot take the form later given by Komen et al. (1984). In spite of its successful use for the estimation of the significant wave height H_s and peak period T_p, these fixed-shape dissipation functions, from Komen et al. (1984) up to (Bidlot et al. 2007), have terrible built-defects, like the spurious amplification of wind sea growth in the presence of swell (Ardhuin et al. 2007), which is contrary to all observations (Violante-Carvalho et al. 2004). Associated with that defect also comes an underestimation of the energy level in the inertial range, making these wave models ill-suited for remote sensing studies, as will be exposed below.

Another widely used formulation has been proposed by Tolman and Chalikov (1996), and some if its features are worth noting. It used a combination of a high frequency dissipation and low frequency dissipation, with a transition at two times the wind sea peak frequency, and a swell attenuation by the wind, here noted $S_{\rm out}$. Yet, its severe underestimation of all source terms yields important biases in wave growth and wave directions at short fetch (Ardhuin et al. 2007). Another parameterization that is successful in some particular conditions are those of Makin and Stam (2003), for high winds, but it fails in moderate sea states (Lefèvre et al. 2004). Polnikov and Inocentini (2008) have also proposed new source term formulations, but the accuracy of their results appears generally less than with the model presented here, in particular for mean periods.

[1] In the presence of variable current, the source of energy for the wave field, i.e. the work of the radiation stresses, is generally eliminated when the energy balance is written as an action balance (e.g. Komen et al. 1994).

Going back to the few available observations of wave dissipation processes, van der Westhuysen et al. (2007) have proposed a dissipation rate proportional to the non-dimensional spectrum,

$$B\left(f\right)=\int_{0}^{2\pi}k^{3}cos^{2}\left(\theta-\theta'\right)F(f,\theta')C_{g}/(2\pi)\mathrm{d}\theta', \tag{4}$$

in the form

$$S_{\mathrm{oc}}\left(f,\theta\right)=-C\sqrt{gk}\left[\frac{B(f)}{B_{r}}\right]^{p/2}, \tag{5}$$

where C is a positive constant, B_r is a constant saturation threshold and and p is a coefficient that varies both with the wind friction velocity $u_\star$ and the degree of saturation $B(f)/B_r$ with, in particular, $p \approx 0$ for $B(f) < 0.8B_r$.

This formulation is an improvement on that proposed by Alves and Banner (2003), because it uses a realistic value for B_r. Yet, for non breaking waves, when $p \approx 0$, the dissipation is too large by at least one order of magnitude, making the parameterization unfit for oceanic scale applications (Ardhuin and Le Boyer 2006). Further, the increase of p with the inverse wave age $u_\star/C$, is designed to produce a given form of high frequency equilibrium rather than letting the equilibrium appear by itself. This increase of S_{oc} at high frequency, needed to obtain a balance with the $S_{\mathrm{atm}} = S_{\mathrm{in}}$ term in equation (1) is also an indication that other factors are important besides the value of the saturation B_r, such as the directionality of the waves (Banner et al. 2002). Other observations clearly show that the breaking rate of high frequency waves is much higher for a given value of B, probably due to cumulative effects by which the longer waves are modifying the dissipation of shorter waves. Banner et al. (1989) and Melville et al. (2002) have shown how breaking waves suppress the short waves on the surface, and we will show here that a simple estimation of the dominant breaking rates based on the observations by Banner et al. (2000) suggests that this effect is dominant for wave frequencies above three times the windsea peak frequency. Young and Babanin (2006) arrived at the same conclusion from the examination of wave spectra, and even proposed a parameterization for S_{oc}. Yet, their interpretation of the differences in parts of a wave record with breaking and non-breaking waves is problematic because the breaking waves have already lost some energy when they are observed and the non-breaking waves are not going to break right after they have been observed. Further, the proposed dissipation rate for the dominant waves is linear in terms of the wave spectrum, which is difficult to reconcile with the observations by Banner et al. (2000) that the breaking probability of dominant waves increases with something that is proportional to the wave spectrum. This would require a rapid decrease of the dissipation rate as the breaking probability increases.

Finally, the recent measurement of swell dissipation by Ardhuin et al. (2009a) has revealed that the dissipation of non-breaking waves is a very important process at scales larger than 1000 km, and is essentially a function of the wave steepness. Because of the differences in coastal and larger scale sea states (e.g. Long and Resio 2007), it is paramount to verify source function parameterizations at all scales, in order to provide a robust and comprehensive parameterization of wave dissipation.

It is thus time to combine the existing knowledge on the dissipation of breaking and non-breaking waves to provide a an improved parameterization for the dissipation of waves. Our objective is to provide a robust parameterization that improves existing wave models. Further work will be needed to further replace the arbitrary choices made here by physically-motivated expressions. We will first present one general form of the dissipation terms that can be made consistent with observed wave dissipation features. The degrees of freedom in this form will then be used to adjust the resulting wave parameters to observations using field experiments and a one year hindcast of waves at the global and regional scale. The model will then be validated with independent data.

2. Parameterizations

Several results will be presented, obtained by a numerical integration of the energy balance. Because numerical choices can have important effects (e.g. Tolman 1992; Hargreaves and Annan 2000), a few details should be given. In the academic uniform ocean case, a minimum time step of 10 s is used, with the adaptative time step scheme of Tolman (2002), and the high frequency tail is left to evolve. Some tests are also done with other parameterizations with a fixed diagnostic tail: namely, above a cut-off frequency f_c the spectrum shape is prescribed, so that the source terms may be out of balance even if there is no spectral evolution.

a. Nonlinear wave wave interactions

All the results discussed and presented in this section are obtained with the Discrete Interaction Approximation of Hasselmann et al. (1985). The coupling coefficient that gives the magnitude of the interactions is C_{nl}. Based on comparisons with exact calculations, Komen et al. (1984) adjusted the value of C_{nl} to 2.78×10^{8}, which is the value used by Bidlot et al. (2005). Here this constant will be allowed to vary slightly.

b. Swell dissipation

Observations of swell dissipation are consistent with the effect of friction at the air-sea interface (Ardhuin et al. 2009a), resulting in a flux of wave momentum from the wave field to the wind (Harris 1966). We thus write the swell dissipation as a negative contribution S_{out} which is thus added to S_{in} to make the wind-wave source term S_{atm}.

The observation by (Ardhuin et al. 2009b) show that that the swell dissipation is non-linear a source function

of the following form was implemented. Defining the boundary Reynolds number Re$= 4u_{\rm orb}a_{\rm orb}/\nu_a$, where $u_{\rm orb}$ and $a_{\rm orb}$ are the significant surface orbital velocity and displacement amplitudes, and ν_a is the air viscosity, we take, for Re less than a critical value Re$_c$

$$S_{\rm out}\left(f,\theta\right) = -C_{\rm dsv}\frac{\rho_a}{\rho_w}\left\{2k\sqrt{2\nu\sigma}\right\}F\left(f,\theta\right), \qquad (6)$$

where $C_{\rm dsv}$ is a constant, equal to 1 in Dore (1978)'s theory. For Re $\geq$Re$_c$ we assume the boundary layer to be turbulent and take

$$S_{\rm out}\left(f,\theta\right) = -\frac{\rho_a}{\rho_w}\left\{16 f_e \sigma^2 u_{\rm orb}/g\right\}F\left(f,\theta\right). \qquad (7)$$

A few tests have indicated that Re$_c = 10^5$ provides reasonable result, although it may be a function of the wind speed. Here we shall use $C_{\rm dsv} = 1.2$, but the result are not too sensitive to variations in the range 0.8 to 1.5.

The parameterization of the turbulent boundary layer is a bit more problematic, and in the absence of direct measurements in the boundary layer, leaves room for speculations. From the analogy with an oscillatory boundary layer over a fixed bottom (Jensen et al. 1989), the values of f_e inferred from the swell observations, in the range 0.004 to 0.013, correspond to a surface with a very small roughness. We also expect the wind speed and direction to influence f_e. We have thus chosen a parameterization form that allows to modify the surface roughness. We also include a correction for wind effects to first order in $u_\star/u_{\rm orb}$,

$$f_e = 0.7 f_{e,GM} + \left[|s_3| + s_2\cos(\theta-\theta_u)\right]u_\star/u_{\rm orb}, \quad (8)$$

where $f_{e,GM}$ is the friction factor given by Grant and Madsen's (1979) theory for rough oscillatory boundary layers without a mean flow. GIVE TYPICAL VALUES OF f_e FOR A/Z0 ... The $O(u_\star/u_{\rm orb})$ correction coefficients s_2 and s_3 coefficient have been adjusted to 0.15 and -0.18, respectively, the latter negative value giving a stronger dissipation for swells opposed to winds. Based on the simple idea that most of the air-sea momentum flux is supported by the pressure-slope correlations that give rise to the wave field (Donelan 1998; Peirson and Banner 2003), we have taken the surface roughness to be a fixed small proportion r_{z0}, here set to 0.04, of the roughness for the wind. This gives a range of values of f_e consistent with the observations, and hindcast swell decay that follow well the observed swell decays for the observed range of swell steepnesses (figure 1).

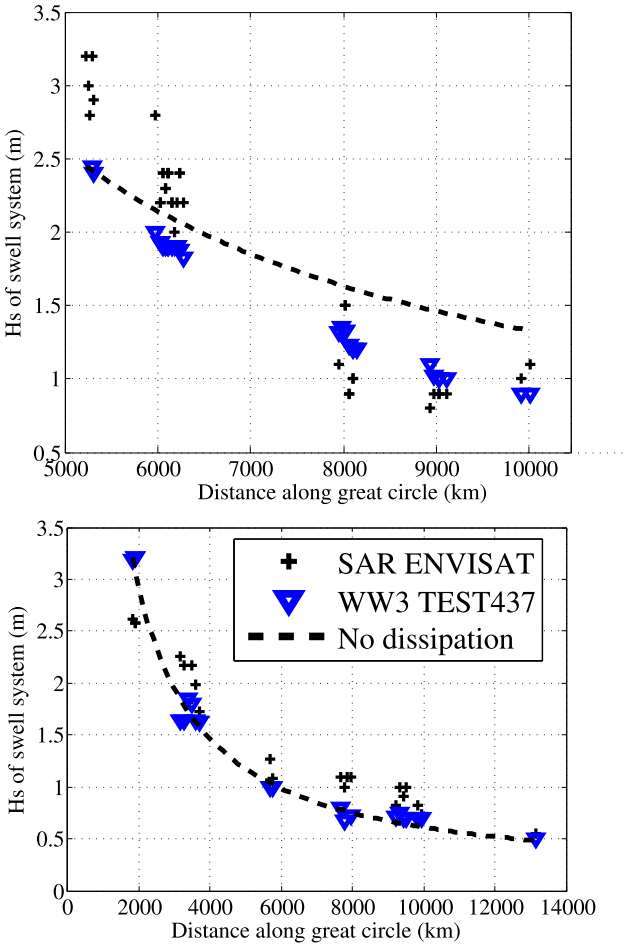

FIG. 1. Comparison of modelled swell significant heights, following the propagation of the two swells shown by Ardhuin et al. (2009a) with peak periods of 15 s and high and low dissipation rates.

c. Wave breaking

Observations show that waves break when the orbital velocity at their crest U_c comes close to the phase speed C, with a ratio $U_c/C > 0.8$ for random waves (Stansell and MacFarlane 2002; Wu and Nepf 2002). The difficulty in the parameterization of breaking is to relate this exceedence of a threshold on the orbital velocity to some parameters derived from the wave spectrum, and to further estimate a spectral rate of energy loss. Also, breaking is intricately related to a complex non-linear evolution of the waves (e.g. Banner and Peirson 2007). We will follow here the more detailed analysis presented in Filipot et al. (2010). Essentially we distiguish a spontaneous breaking from an induced breaking, the latter being caused by large scale breakers overtaking shorter waves, and causing them to be dissipated. For the spontaneous breaking we parameterize the dissipation rate directly from the spectrum, without the intermediate step of estimating a breaking probability.

We started from the simplest possible dissipation term formulated in terms of the direction-integrated spectral saturation $B\left(f\right)$

$$B_0\left(f,\theta\right) = \int_0^{2\pi} k^3 F(f,\theta')C_g/(2\pi)\mathrm{d}\theta', \qquad (9)$$

for which a realistic threshold $B_{0r} = 1.2\times10^{-3}$ cor-

responding to the onset of wave breakingBabanin and Young (2005). This saturation parameter corresponds exactly the α parameter defined by Phillips (1958), an which was initially thought to be constant at high frequency, corresponding to a self-similar sea state in which waves of all scales have the same shape, dictated by the breaking limit.

Early tests and comparison against directional spectra indicated that the spectra were too narrow (Ardhuin and Le Boyer 2006). This effect could be due to many errors, but, because Babanin et al. (2001) introduced a directional width in their saturation, we similarly modified the definition of B. Expecting also to have different dissipation rates in different directions, we defined a saturation that would correspond, in deep water, to a normalized velocity variance projected in one direction, with a further restriction of the integration of directions.

$$B'\left(f,\theta\right)=\int_{\theta-\Delta_\theta}^{\theta+\Delta_\theta}k^3cos^2\left(\theta-\theta'\right)F(f,\theta')C_g/(2\pi)\mathrm{d}\theta', \tag{10}$$

Here we shall always use $\Delta_\theta = 80^\circ$. As a result a sea state with two systems of same energy but opposite direction will typically produce much less dissipation that a sea state with all the energy radiated in the same direction. This is debatable, but it appeared to us more robust that using B_0 divided by the directional width, as done by Babanin et al. (2001) and Banner et al. (2002), since this would even further reduce the dissipation in such a case.

We then define our dissipation term as the sum of the saturation-based term of Ardhuin et al. (2008) and a cumulative breaking term $S_{\rm bk,cu}$ adapted from Filipot et al. (2008), form

$$\begin{aligned}S_{\rm oc}(f,\theta) &= \sigma C_{\rm ds}^{\rm sat}\left\{0.25\left[\max\left\{\tfrac{B(f)}{B_r'}-1,0\right\}\right]^2\right.\\ &\left.+0.75\left[\max\left\{\tfrac{B'(f,\theta)}{B_r'}-1,0\right\}\right]^2\right\}\\ &\times F(f,\theta)+S_{\rm bk,cu}(f,\theta)+S_{\rm turb}(f,\theta).\end{aligned} \tag{11}$$

where

$$B'\left(f,\theta\right)=\int_{\theta-80^\circ}^{\theta+80^\circ}k^3cos^2\left(\theta-\theta'\right)F(f,\theta')C_g/(2\pi)\mathrm{d}\theta', \tag{12}$$

$$B\left(f\right)=\max\left\{B'(f,\theta),\theta\in[0,2\pi[\right\}. \tag{13}$$

The dissipation $S_{\rm turb}$ due to wave-turbulence interactions is expected to be much weaker (Ardhuin and Jenkins 2006) and will be neglected here.

Finally, following the analysis by Filipot et al. (2010), the threshold B_r is corrected for shallow water, so that B'/B_r' in different water depths correspond to the same ratio of the root mean square orbital velocity and phase speed. For periodic and irrotational waves, the orbital velocity increases much more rapidly than the wave height as it approaches the breaking limit. Further, due to nonlinear distortions in the wave profile in shallow water, the height can be twice as large as the height of linear waves with the same energy. In order to express a relevant threshold from the elevation variance, we consider the slope $kH_{\rm lin}(kD)$ of an hypothetical linear wave that has the same energy as the wave of maximum height. In deep water, $kH_{\rm lin}(\infty)\approx 0.77$, and for other water depths we thus correct B_r by a factor $(kH_{\rm lin}(kD)/H_{\rm lin}(\infty))^2$. Using streamfunction theory (Dalrymple 1974), a polynomial fit as a function of $Y=\tanh(kD)$ gives

$$B_r'=B_rY\left[M_4Y^3+M_3Y^2+M_2Y+M_1\right]. \tag{14}$$

such that $B_r'=B_r$ in deep water. The fitted constants are $M_4=1.3286$, $M_3=-2.5709$, $M_2=1.9995$ and $M_1=0.2428$. Although this behaviour is consistent with the variation of the depth-limited breaking parameter γ derived empirically by Ruessink et al. (2003), the resulting dissipation rate is not yet expected to produce realistic results for surf zones because no effort was made to verify this aspect. This is the topic of ongoing work, outside of the scope of the present paper.

When including the normalization by the width of the directional spectrum (here replaced by the $\cos^2$ factor in eq. 12), $B_r = 0.0009$ is a threshold for the onset of breaking consistent with the observations of Banner et al. (2000) and Banner et al. (2002), as discussed by Babanin and van der Westhuysen (2008). The dissipation constant $C_{\rm ds}^{\rm sat}$ was adjusted to 2.2×10^{-4} in order to reproduce the directional fetch-limited data described by Ardhuin et al. (2007).

The cumulative breaking term $S_{\rm bk,cu}$ represents the smoothing of the surface by big breakers with celerity C' that wipe out smaller waves of phase speed C. Due to uncertainties in the estimation of this effect in the observations of Young and Babanin (2006), we use the theoretical model of Ardhuin et al. (2009b), with a simple numerical correction. Briefly, the relative velocity of the crests is the norm of the vector difference, $\Delta_C=|\mathbf{C}-\mathbf{C}'|$, and the dissipation rate of short wave is simply the rate of passage of the large breaker over short waves, i.e. the integral of $\Delta_C\Lambda(\mathbf{C})d\mathbf{C}$, where $\Lambda(\mathbf{C})d\mathbf{C}$ is the length of breaking crests per unit surface that have velocity components between C_x and C_x+dC_x, and between C_y and C_y+dC_y (Phillips 1985). Because there is no consensus on the form of Λ (Gemmrich et al. 2008), we prefer to link Λ to breaking probabilities. Based on Banner et al. (2000, figure 6), and taking their saturation parameter ε to be of the order of $1.6\sqrt{B}$, the breaking probability of dominant waves waves is approximately $P=56.8\left(\max\{\sqrt{B}-\sqrt{B_r},0\}\right)^2$. However, because they used a zero-crossing analysis, for a given wave scale, there are many times when waves are not counted because the record is dominated by another scale. This tends to overestimate the breaking probability by a factor of 2. We shall thus correct for this effect, simply dividing P by 2. Extrapolating this result to higher frequencies, and assuming that the spectral density of crest length per

unit surface $l(\mathbf{k})$, in the wavenumber spectral space, is $l(\mathbf{k}) = 1/(2\pi^2 k)$, we define a spectral density of breaking crest length, $\Lambda(\mathbf{k}) = l(\mathbf{k})P(\mathbf{k})$, giving the source term,

$$S_{\rm bk,cu}(f,\theta) = -C_{\rm cu}F(f,\theta)\int_0^{f\times r_{cu}}\int_0^{2\pi}\frac{28.4}{\pi} \times \max\left\{\sqrt{B(f',\theta'}-\sqrt{B_r},0\right\}\frac{\Delta_C}{C_g'}{\rm d}\theta'{\rm d}f', \quad (15)$$

where r_{cu} defines the maximum ratio of the frequencies of long waves that will wipe out short waves. We shall take $r_{cu} = 0.5$, and $C_{\rm cu}$ is a tuning coefficient expected to be of order 1.

As shown in figure 2, a reasonable balance is obtained for $C_{\rm cu} = 1$. Compared the the source term balance given by Bidlot et al. (2005) (hereinafter BAJ), the nonlinear interactions are much smaller at high frequency, essentially because the spectrum approaches a f^{-4} shape, whereas with BAJ it decreases even faster than f^{-5} when the tail is left to evolve freely (figure 3). However, for strongly forced conditions the dominant waves break frequently, and $C_{\rm cu} = 1$ reduces the energy level in the tail below observed levels. This effect can be seen by considering satellite-derived mean square slopes (figure 4), or high moments of the frequency spectrum derived from buoy data.

That effect can be mitigated by decreasing $C_{\rm cu}$ or increasing $r_{\rm cu}$, so that dominant breaking waves will only wipe out much smaller waves. Instead, and because the wind to wave momentum flux was apparently too high in high winds, we chose to introduce one more degree of freedom, allowing a reduction of the wind input at high frequency.

d. Wind input

The wind input parameterization is slightly adapted from Janssen (1991) and the following adjustments performed by Bidlot et al. (2005, 2007). Thus the full wind input source term reads

$$S_{\rm in}(f,\theta) = S_{\rm in}^{\rm up}(f,\theta) + \frac{\rho_a}{\rho_w}\frac{\beta_{\max}}{\kappa^2}{\rm e}^Z Z^4\left(\frac{u_\star}{C}\right)^2 \max\left\{\cos(\theta-\theta_u),0\right\}^p \sigma F(f,\theta), \quad (16)$$

where $\beta_{\max}$ is a non-dimensional growth parameter (constant), κ is von Kármán's constant. In the present implementation the air/water density ratio is constant. The power of the cosine is taken constant with $p = 2$. We define $Z = \log(\mu)$ where μ is given by Janssen (1991), and corrected for intermediate water depths, so that

$$Z = \log(kz_1) + \kappa/\left[\cos(\theta-\theta_u)(u_\star/C + z_\alpha)\right], \quad (17)$$

where z_1 is a roughness length modified by the wave-supported stress τ_w, and z_α is a wave age tuning parameter. z_1 is implicitly defined by

$$U_{10} = \frac{u_\star}{\kappa}\log\left(\frac{z_u}{z_1}\right) \quad (18)$$

$$z_0 = \max\left\{\alpha_0\frac{\tau}{g}, z_{0,\max}\right\} \quad (19)$$

$$z_1 = \frac{z_0}{\sqrt{1-\tau_w/\tau}}. \quad (20)$$

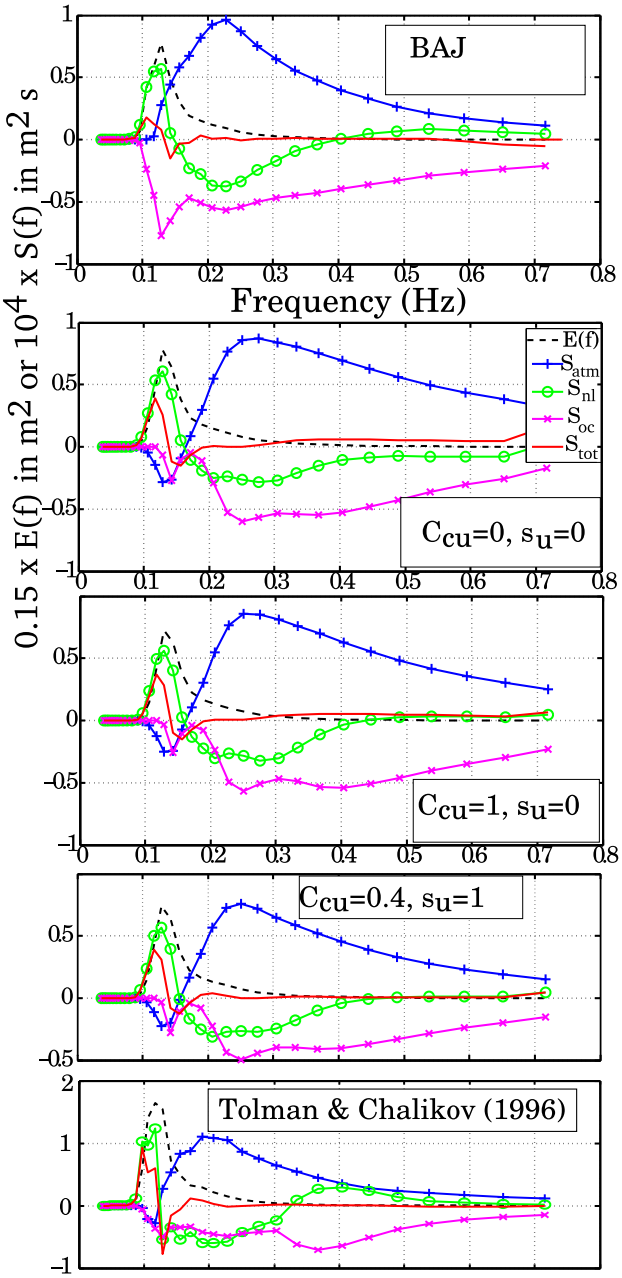

FIG. 2. Academic test case over a uniform ocean with a uniform 10 m s^{-1} wind. Source term balances given by the parameterization of (Bidlot et al. 2005, , 'BAJ'), and the parameterizations proposed here with the successive introduction of the cumulative breaking and the wind sheltering effects with the parameters C_{cu} and s_u. For BAJ, a diagnostic f^{-5} tail is applied above 2.5 the mean frequency.)

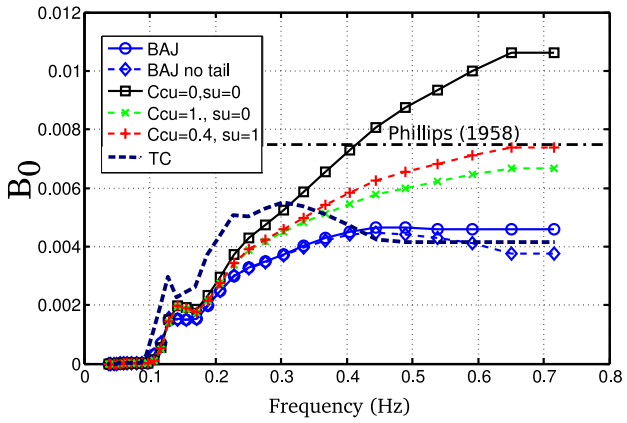

FIG. 3. Values of the spectral saturation B_0 for the cases presented in figure 2.

The maximum value of z_0 was added to reduce the unrealistic stresses at high winds that are otherwise given by the standard parameterization. We take $z_{0,\max} = 0.0015$, which is equivalent to setting a maximum wind drag coefficient of 2.5×10^{-3}. We further have adjusted $z_\alpha = 0.006$ and $\beta_{\max} = 1.52$.

An important part of the parameterization is the calculation of the wave-supported stress τ_w, which includes the resolved part of the spectrum, as well as the growth of an assumed f^{-5} diagnostic tail beyond the highest frequency. This parameterization is highly sensitive to the high frequency part of the spectrum since a high energy level there will lead to a larger value of $u_\star$ and thus positive feedback on the wind input via z_1. In the present implementation, an ad hoc and optional reduction of $u_\star$ is implemented in order to allow a balance with a saturation-based dissipation. This correction also reduces the drag coefficient at high winds. Essentially, the wind input is reduced for high frequencies and high winds, loosely following Chen and Belcher (2000). This is performed by replacing $u_\star$ is eq. (16) with $u'_\star(k)$ defined for each frequency as

$$\begin{aligned}\left(u'_\star\right)^2 &= u_\star^2\left(\cos\theta_u, \sin\theta_u\right) \\ &- |s_u| \int_0^k \int_0^{2\pi} \frac{S_{in}\left(f',\theta\right)}{C}\left(\cos\theta, \sin\theta\right) \mathrm{d}f'\mathrm{d}\theta,\end{aligned} \tag{21}$$

where the sheltering coefficient $|s_u| \sim 1$ can be used to tune the stresses at high winds, which would be largely overestimated for $s_u = 0$. For $s_u > 0$ this sheltering is also applied within the diagnostic tail, which requires the estimation of a 3-dimensional look-up table for the high frequency stress.

3. Consequences of the source term shape

The presence of a cumulative dissipation term allows a different balance in the spectral regions above the peak, where an inertial range with a spectrum proportional to f^{-4} develops, and the high frequency tail were the spectrum decays like f^{-5} or possibly a little faster. The spectral level in the range 0.2 to 0.4 Hz was carefully compared against buoy data, where is was found to be realistic. In particular we have investigated the systematic variation of spectral moments

$$m_n(f_c) = \int_0^{f_c} f^n E(f) \mathrm{d}f. \tag{22}$$

with $n =$ 2,3 and 4, and cut-off frequencies in the range 0.2 to 0.4 Hz. Such moments are relevant to a variety of applications. Ardhuin et al. (2009b) investigated the third moment, which is proportional to the surface Stokes drift in deep water, and found that buoy data are very well represented by a simple function, which typically explains 95% of the variance,

$$\begin{aligned} m_3(f_c) &\simeq \frac{5.9g}{(2\pi)^3} \times 10^{-4}\left[1.25 - 0.25\left(\frac{0.5}{f_c}\right)^{1.3}\right] U_{10} \\ &\times \min\left\{U_{10}, 14.5\right\} + 0.027\left(H_s - 0.4\right), \end{aligned} \tag{23}$$

where f_c is in Hertz, U_{10} is in meters per second, and H_s is in meters.

This relationship is well reproduced in hindcasts using $C_{\mathrm{cu}} = 0.4$ and $s_u = 1$, while the BAJ source terms give almost a a constant value of m_3 for any wind speed (Ardhuin et al. 2009b). Here we also consider the fourth moment m_4, which, for linear waves is proportional to a surface mean square slope filtered at the frequency f_c. Figure 4 shows that for any given wind speed mss_C increases with the wave height (Gourrion et al. 2002), whereas this is not the case of m_4 in the BAJ parameterization, or, for very high winds, when C_{cu} is too strong. In the case of BAJ, this is due to the $(k/k_x)^2$ part in the dissipation term (eq. 2), which plays a role similar to the cumulative term in our formulation. For $C_{\mathrm{cu}} = 1$ and $s_u = 0$, the cumulative effect gets too strong for wind speeds over 10 m s^{-1}, in which case m_4 starts to decrease with increasing wave height, whereas for high winds and low (i.e. young) waves, the high frequency tail is too high and m_4 gets as large as 6%, which is unrealistic. It thus appears, that the high frequency tail, for $s_u = 0$, responds too much to the wind, hence our use of $s_u = 1$ in most of the following simulations.

This interpretation of the model result assumes that the high frequency part of the spectrum can be simply converted to a wavenumber spectrum. This is not exactly the case as demonstrated by Banner et al. (1989). Also, there is no consensus on the nature of the spectrum modelled with the energy balance equation but, since non-resonant nonlinearities are not represented, the modelled spectra are expected to be more related to Lagrangian buoy measurements, rather than Eulerian measurements. This mat-

ter is left for further studies, together with a detailed interpretation of altimeter radar cross sections. Although the number of data is not as large, the use of buoy data produces results entirely similar to figure 4. ...

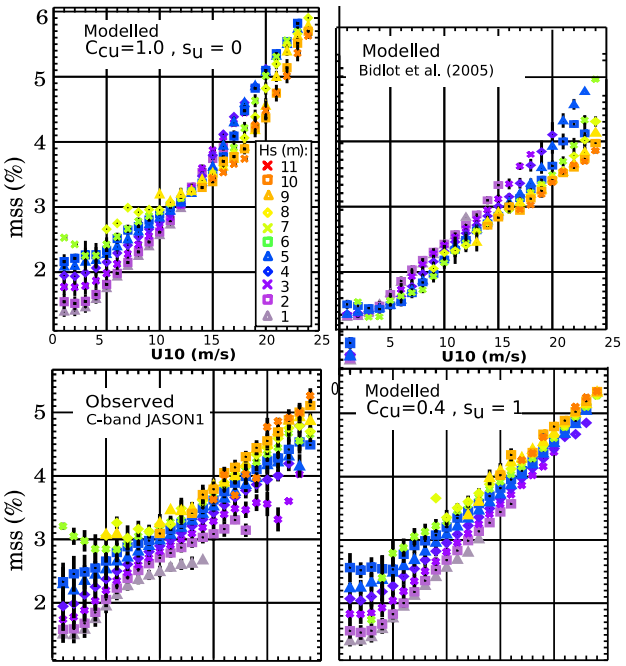

FIG. 4. Variation of the surface mean square slope estimated as either $0.64/\sigma_0$ using the C-band altimeter on board JASON-1, after the correction of a 1.2 dB bias in the JASON data, or by integration of modelled spectra from 0 to 0.72 Hz, with either the $C_{cu} = 0.4$ and $s_u = 1$ parameterization (TEST441) or the parameterization by Bidlot et al. (2005). For modelled values a constant 0.011 is added to account for the short waves that contribute to the satellite signal and that are not resolved in the model. This saturated high frequency tail is consistent with the observations of Vandemark et al. (2004). The original 1 Hz data from JASON is subsampled at 0.5 Hz and averaged over 10 s, namely 58 km along the satellite track. The same averaging is applied to the wave model result, giving the 393382 observations reported here, for the first half year of 2007.

4. Verification

In order to provide simplified measures of the difference between model and observations we use the following definitions for the normalized root mean square error (NRMSE) , the bias (or should we also use a normalized bias ...?) and the correlation coefficient. The use of NRMSE instead of RMSE allows a quantitative comparison between widely different sea state regimes. Because previous studies have often used RMSE we also provide RMSE values....

a. Slanting fetch limited growth

SHOWEX ... model resolution here is 1/50 degree (1.5 km)... a bit too coarse for the coastal part. I'll redo the calculations with finer resolution and Aaron's unstructured scheme, which will also allow a XNL calculation (may not for this paper ...).

FIG. 5. Fetch-limited growth for the SHOWEX case discussed in Ardhuin et al. (2007).

FIG. 6. Model-data comparison at buoys X2 during the SHOWEX event discussed in Ardhuin et al. (2007).

Because the strength of the source terms is constrained by the mean direction as a function of frequency and the difference Sin-Sds is constrained by the growth curve E(X), one can only change the shape of the source terms in order to fit the observed directional spread. This can be done by either making the wind input broader (apparently not very effective) or by reducing the dissipation rate of waves propagating at large oblique angles. In the present parameterization this is controlled by Δ_θ. WARNING: the SHOWEX calculations use a directional resolution of 10 whereas my global runs used 15: the impact of this has to be checked! Here are shown for comparisons two tests with different values of Δ_θ. The error on the directional spread at all SHOWEX buoys is largely reduced for $\Delta_\theta = 70°$.

b. Global scale results

In situ measurements gathered for the model verification project of the IOC-WMO Joint Commission on Oceanography and marine Meteorology (JCOMM) are used here in order to provide an extensive coverage of the ocean basins (MUST ADD THE PERU BUOY). The exchanged data includes only the significant wave heights H_s and a measure of the period, either the peak period T_p or the mean period

... Buoy data close to coast, validation more general for Hs with altimeters ... both are coherent. Add a table with statistics for a few lists of buoys (FIRST, ... ?). Need to add decay along swell tracks for the verification of the swell dissipation term.

FIG. 7. Statistics for the year 2007. NRMSE for (a) H_s and (b) T_p or T_{m02} at in situ locations (T_p is shown at all buoys except U.K. and French buoys for which T_{m02} is shown). Symbols ∇, $\triangle$, $\circ$, square, and diamond correspond to values in the ranges $0 \le x < 10$, $10 \le x < 20$, $20 \le x < 30$, $30 \le x < 40$, $40 \le x$. (c) bias for periods in seconds. Symbols ∇, $\triangle$, $\circ$, Box, diamond and $\star$ correspond to values in the ranges $x < -1$, $-1 \le x < -0.5$, $-0.5 \le x < 0$, $0 \le x < 0.5$, $0.5 \le x < 1$, $1 \le x$, respectively.

c. Hindcast of the 2004 U.S. East coast hurricane season??

Redo the case used by Aaron for test of WWM ... check n wind quality first? use ECMWF or NCEP's NAH winds??

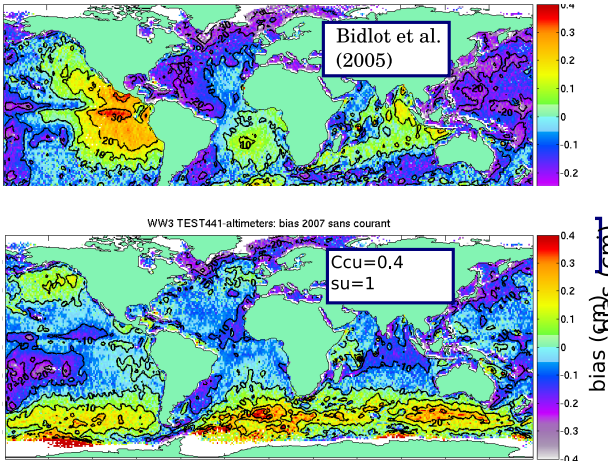

FIG. 8. Bias for the year 2007 in centimeters. The global 0.5 WWATCH model is compared to altimeters JASON, ENVISAT and GFO following the method of Rascle et al. (2008). The top panel is the result with the BAJ parameterization, and the bottom panel is the result with the $C_{cu} = 0.4$ and $s_u = 1$ (TEST441) parameterization.

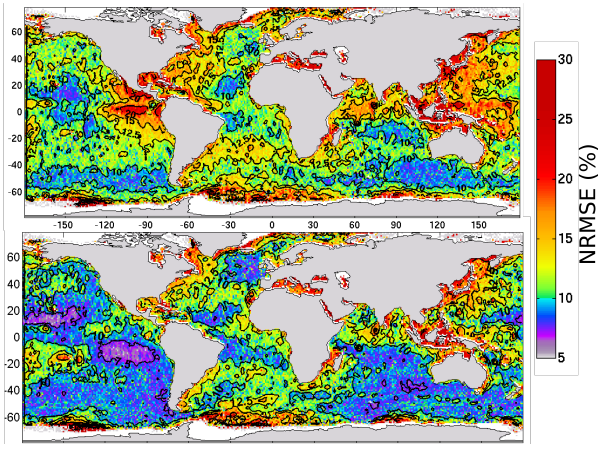

FIG. 9. Normalized RMSE for the year 2007 in percents. The global 0.5 WWATCH model is compared to altimeters JASON, ENVISAT and GFO following the method of Rascle et al. (2008). The top panel is the result with the BAJ parameterization, and the bottom panel is the result with the $C_{cu} = 0.4$ and $s_u = 1$ (TEST441) parameterization.

5. Conclusions

it works but ...

Acknowledgments. This research would not have been possible without the dedication of Hendrik Tolman and Arun Chawla in putting together the core of the WAVEWATCH III code. Florent Birrien performed the integration of Aaron Roland's routines into the WAVEWATCH III framework. Wind and wave data were kindly provided by ECMWF, Météo-France, and the French Centre d'Etudes Techniques Maritimes Et Fluviales (CETMEF). The SHOM buoy deployments were managed by David Corman with precious help from Guy Amis.

APPENDIX A **Parameter settings in WAVEWATCH III**

All parameters defining the dissipation source function and their numerical values are listed in table A1 for the wind-wave interaction term $S_{\rm atm}$ and table A2 for the wave-ocean interaction term $S_{\rm oc}$. We also recall that the nonlinear coupling coefficient (variable NLPROP in WWATCH) is set to 2.78×10^8 in all cases, except for the two parameterizations mostly used here, with $C_{\rm nl} = 2.5 \times 10^8$ in TEST437 and TEST441. Although the best performance for most parameters is obtained with the TEST441 settings, its underestimation of extreme sea states may be a problem in some applications for which the TEST437 may be preferred. A full tuning of the model has not been tried yet and it is possible that a simple adjustment of $C_{\rm cu}$, r_{cu} and s_u may produce even better results. Finally, these parameters have been mostly adjusted for deep water conditions using ECMWF winds. Using other sources of winds for large scale applications may require a retuning of the wind source function, which can be best performed by a readjustment of $\beta_{\rm max}$.

REFERENCES

Alves, J. H. G. M. and M. L. Banner, 2003: Performance of a saturation-based dissipation-rate source term in modeling the fetch-limited evolution of wind waves. *J. Phys. Oceanogr.*, **33**, 1274–1298.

Ardhuin, F., B. Chapron, and F. Collard, 2009a: Observation of swell dissipation across oceans. *Geophys. Res. Lett.*, **in press**. http://hal.archives-ouvertes.fr/hal-00321581/

Ardhuin, F., F. Collard, B. Chapron, P. Queffeulou, J.-F. Filipot, and M. Hamon, 2008: Spectral wave dissipation based on observations: a global validation. *Proceedings of Chinese-German Joint Symposium on Hydraulics and Ocean Engineering, Darmstadt, Germany*, 391–400.

Ardhuin, F., T. H. C. Herbers, K. P. Watts, G. P. van Vledder, R. Jensen, and H. Graber, 2007: Swell and slanting fetch effects on wind wave growth. *J. Phys. Oceanogr.*, **37**, doi:\bibinfo{doi}{10.1175/JPO3039.1}, 908–931.

Ardhuin, F. and A. D. Jenkins, 2006: On the interaction of surface waves and upper ocean turbulence. *J. Phys. Oceanogr.*, **36**, 551–557.

Ardhuin, F. and A. Le Boyer, 2006: Numerical modelling of sea states: validation of spectral shapes (in French). *Navigation*, **54**, 55–71.

Ardhuin, F., L. Marié, N. Rascle, P. Forget, and A. Roland, 2009b: Observation and estimation of Lagrangian, Stokes and Eulerian currents induced by wind and waves at the sea surface. *J. Phys. Oceanogr.*, submitted, available at http://hal.archives-ouvertes.fr/hal-00331675/.

Babanin, A., I. Young, and M. Banner, 2001: Breaking probabilities for dominant surface waves on water of finite depth. *J. Geophys. Res.*, **106**, 11659–11676.

Babanin, A. V. and A. J. van der Westhuysen, 2008: Physics of saturation-based dissipation functions proposed for wave forecast models. *J. Phys. Oceanogr.*, **38**, 1831–1841. http://ams.allenpress.com/archive/1520-0485/38/8/pdf/i1520-0485-38-8-1831

Babanin, A. V. and I. R. Young, 2005: Two-phase behaviour of the spectral dissipation of wind waves. *Proceedings of the 5th International Symposium Ocean Wave Measurement and Analysis, Madrid, june 2005*, ASCE, paper number 51.

Paramtre	variable dans WWATCH.	WAM-Cycle4	BAJ	TEST405	TEST441	TEST437
α_0	ALPHA0	0.01	0.0095	0.0095	0.0095	0.0095
$\beta_{\max}$	BETAMAX	1.2	1.2	1.55	1.52	1.52
z_α	ZALP	0.0110	0.0110	0.006	0.006	0.006
s_u	TAUWSHELTER	0.0	0.0	0.0	0.0	1.0
s_0	SWELLFPAR	0	0	3	3	3
s_1	SWELLF	0.0	0.0	0.8	0.7	0.7
s_2	SWELLF2	0.0	0.0	-0.18	-0.18	-0.18
s_3	SWELLF3	0.0	0.0	0.15	0.15	0.15
Re_c	SWELLF4	0.0	0.0	10^5	10^5	10^5
C_{dsv}	SWELLF5	0.0	0.0	1.2	1.2	1.2
z_r	Z0RAT	0.0	0.0	0.04	0.04	0.04

Table A1. Wind-wave interaction parameters as implemented in version 3.14-SHOM of the WAVEWATCH III code, and values used in the tests presented here. In WWATCH, all parameters are accessible via the SIN3 namelist. All of these parameters are included in version 3.14 of WWATCH. s_0 is a switch that, if nonzero, activates the calculation of S_{out}.

Parameter	variable in WWATCH	WAM4	BAJ	TEST405	TEST437	TEST441
C_{ds}	SDSC1	-4.5	-2.1	0.0	0.0	0.0
p	WNMEANP	-0.5	0.5	0.5	0.5	0.5
p_{tail}	WNMEANPTAIL	-0.5	0.5	0.5	0.5	0.5
f_{FM}	FXFM3	2.5	2.5	2.5	9.9	9.9
δ_1	SDSDELTA1	0.5	0.4	0.0	0.0	0.0
δ_2	SDSDELTA2	0.5	0.6	0.0	0.0	0.0
$C_{\mathrm{ds}}^{\mathrm{sat}}$	SDSC2	0.0	0.0	-2.4×10^{-5}	-2.4×10^{-5}	-2.4×10^{-5}
C_{lf}	SDSLF	1.0	1.0	0.0	0.0	0.0
C_{hf}	SDSHF	1.0	1.0	0.0	0.0	0.0
Δ_θ	SDSDTH	0.0	0.0	80	80	80
B_r	SDSBR	0.0	0.0	1.2×10^{-3}	9×10^{-4}	9×10^{-4}
p^{sat}	SDSP	0.0	0.0	2.0	2.0	2.0
r_{cu}	SDSBRF1	0.0	0.0	0.0	0.5	0.5
$2 * C_{\mathrm{cu}}$	SDSC3	0.0	0.0	0.0	2.0	0.8
C_{turb}	SDSC5	0.0	0.0	0.0	0.0	0.0
M_0	SDSBM0	0.0	0.0	1.0	1.0	1.0
M_1	SDSBM1	0.0	0.0	0.2428	0.2428	0.2428
M_2	SDSBM2	0.0	0.0	1.9995	1.9995	1.9995
M_3	SDSBM3	0.0	0.0	-2.5709	-2.5709	-2.5709
M_4	SDSBM4	0.0	0.0	1.3286	1.3286	1.3286

Table A2. Dissipation parameter as implemented in version 3.14-SHOM of the WAVEWATCH III code, and values used in the tests presented here. In WWATCH, all parameters are accessible via the SDS3 namelist. Most of these are also included in version 3.14, except for C_{cu} which is needed for the TEST437 and TEST441 with results described here. The TEST405 can be ran with version 3.14. The parameter m_0 is a switch for the correction or not of B_r into B_r', when $m_0 = 1$, as is the case here, the correction is not applied.

Banner, M. L., A. V. Babanin, and I. R. Young, 2000: Breaking probability for dominant waves on the sea surface. *J. Phys. Oceanogr.*, **30**, 3145–3160. http://ams.allenpress.com/archive/1520-0485/30/12/pdf/i1520-0485-30-12-3145.pdf

Banner, M. L., J. R. Gemmrich, and D. M. Farmer, 2002: Multiscale measurement of ocean wave breaking probability. *J. Phys. Oceanogr.*, **32**, 3364–3374. http://ams.allenpress.com/archive/1520-0485/32/12/pdf/i1520-0485-32-12-3364.pdf

Banner, M. L., I. S. F. Jones, and J. C. Trinder, 1989: Wavenumber spectra of short gravity waves. *J. Fluid Mech.*, **198**, 321–344.

Banner, M. L. and W. L. Peirson, 2007: Wave breaking onset and strength for two-dimensional deep-water wave groups. *J. Fluid Mech.*, **585**, 93–115.

Bidlot, J., S. Abdalla, and P. Janssen, 2005: A revised formulation for ocean wave dissipation in CY25R1. Technical Report Memorandum R60.9/JB/0516, Research Department, ECMWF, Reading, U. K.

Bidlot, J., P. Janssen, and S. Abdalla, 2007: A revised formulation of ocean wave dissipation and its model impact. Technical Report Memorandum 509, ECMWF, Reading, U. K.

Cavaleri, L., 2006: Wave modeling where to go in the future. *Bull. Amer. Meterol. Soc.*, **87**, 207–214. http://ams.allenpress.com/pdfserv/10.1175%2FBAMS-87-2-207

Chen, G. and S. E. Belcher, 2000: Effects of long waves on wind-generated waves. *J. Phys. Oceanogr.*, **30**, 2246–2256.

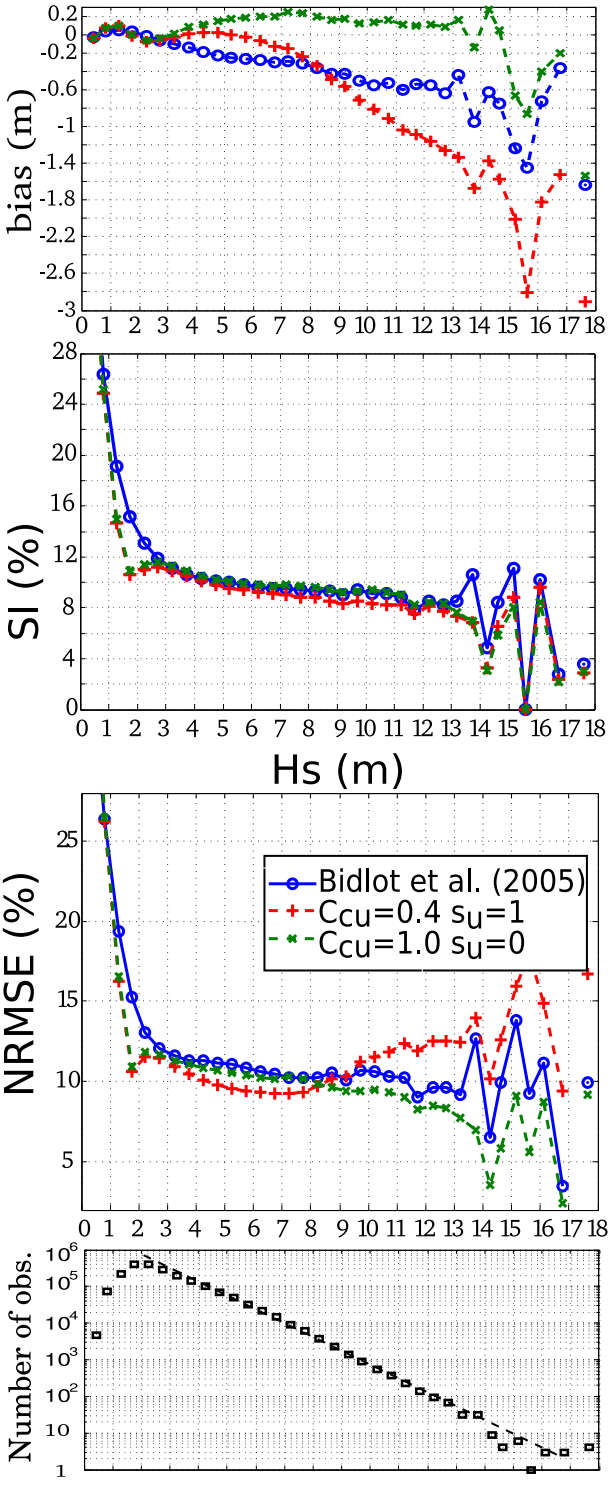

FIG. 10. Wave model errors as a function of H_s. All model parameterizations are used in a global WWATCH model settings using a 0.5° resolution. The model output at 3h intervals is compared to JASON, ENVISAT and GFO following the method of Rascle et al. (2008). Namely, the altimeter 1 Hz Ku band estimates of H_s are averaged over 0.5^circ to match the wave model resolution (Pierre please confirm ...). After this averaging, the total number of observations is 2044545.

Dalrymple, R. A., 1974: A finite amplitude wave on a linear shear current. *J. Geophys. Res.*, **79**, 4498–4504.

Donelan, M. A., 1998: Air-water exchange processes. *Physical Processes in Lakes and Oceans*, J. Imberger, ed., American Geophysical Union, Washington, D.C., pages 18–36, iSBN 0-87590-268-5.

Dore, B. D., 1978: Some effects of the air-water interface on gravity waves. *Geophys. Astrophys. Fluid. Dyn.*, **10**, 215–230.

Filipot, J.-F., F. Ardhuin, and A. Babanin, 2008: Paramétrage du déferlement des vagues dans les modèles spectraux : approches semi-empirique et physique. *Actes des Xèmes journées Génie côtier-Génie civil, Sophia Antipolis*, Centre Français du Littoral.

— 2010: A unified spectral wave breaking dissipation formulation. Part 1. Breaking probability. *J. Geophys. Res.*, **52**, in preparation.

Gelci, R., H. Cazalé, and J. Vassal, 1957: Prévision de la houle. La méthode des densités spectroangulaires. *Bulletin d'information du Comité d'Océanographie et d'Etude des Côtes*, **9**, 416–435.

Gemmrich, J. R., M. L. Banner, and C. Garrett, 2008: Spectrally resolved energy dissipation rate and momentum flux of breaking waves. *J. Phys. Oceanogr.*, **38**, 1296–1312. http://ams.allenpress.com/archive/1520-0485/38/6/pdf/i1520-0485-38-6-1296

Gourrion, J., D. Vandemark, S. Bailey, and B. Chapron, 2002: Investigation of C-band altimeter cross section dependence on wind speed and sea state. *Can. J. Remote Sensing*, **28**, 484–489.

Grant, W. D. and O. S. Madsen, 1979: Combined wave and current interaction with a rough bottom. *J. Geophys. Res.*, **84**, 1797–1808.

Hargreaves, J. C. and J. D. Annan, 2000: Comments on –improvement of the short-fetch behavior in the wave ocean model (WAM)–. *J. Atmos. Ocean Technol.*, **18**, 711–715. http://ams.allenpress.com/archive/1520-0426/18/4/pdf/i1520-0426-18-4-711.pdf

Harris, D. L., 1966: The wave-driven wind. *J. Atmos. Sci.*, **23**, 688–693.

Hasselmann, K., 1974: On the spectral dissipation of ocean waves due to white capping. *Boundary-Layer Meteorol.*, **6**, 107–127.

Hasselmann, S., K. Hasselmann, J. Allender, and T. Barnett, 1985: Computation and parameterizations of the nonlinear energy transfer in a gravity-wave spectrum. Part II: Parameterizations of the nonlinear energy transfer for application in wave models. *J. Phys. Oceanogr.*, **15**, 1378–1391.

Janssen, P. A. E. M., 1991: Quasi-linear theory of of wind wave generation applied to wave forecasting. *J. Phys. Oceanogr.*, **21**, 1631–1642, see comments by D. Chalikov, J. Phys. Oceanogr. 1993, vol. 23 pp. 1597–1600. http://ams.allenpress.com/archive/1520-0485/21/11/pdf/i1520-0485-21-11-1631.pdf

Jensen, B. L., B. M. Sumer, and J. Fredsøe, 1989: Turbulent oscillatory boundary layers at high Reynolds numbers. *J. Fluid Mech.*, **206**, 265–297.

Komen, G. J., L. Cavaleri, M. Donelan, K. Hasselmann, S. Hasselmann, and P. A. E. M. Janssen, 1994: *Dynamics and modelling of ocean waves*. Cambridge University Press, Cambridge, 554 pp.

Komen, G. J., K. Hasselmann, and S. Hasselmann, 1984: On the existence of a fully developed windsea spectrum. *J. Phys. Oceanogr.*, **14**, 1271–1285. http://ams.allenpress.com/archive/1520-0485/14/8/pdf/i1520-0485-14-8-1271.pdf

Lefèvre, J.-M., S. E. Ştefănescu, and V. Makin, 2004: Implementation of new source terms in a third generation wave model. *Preprints of the 3th International workshop on wave hindcasting and forecasting, Montreal, Quebec, 19-22 May*, Environment Canada.

Long, C. E. and D. T. Resio, 2007: Wind wave spectral observations in Currituck Sound, North Carolina. *J. Geophys. Res.*, **112**, doi: \bibinfo{doi}{10.1029/2006JC003835}, C05001.

Makin, V. K. and M. Stam, 2003: New drag formulation in NEDWAM. Technical Report 250, Koninklijk Nederlands Meteorologisch Instituut, De Bilt, The Netherlands.

Melville, W. K., F. Verron, and C. J. White, 2002: The velocity field under breaking waves: coherent structures and turbulence. *J. Fluid Mech.*, **454**, 203–233.

Peirson, W. L. and M. L. Banner, 2003: Aqueous surface layer flows induced by microscale breaking wind waves. *J. Fluid Mech.*, **479**, 1–38.

Phillips, O. M., 1958: The equilibrium range in the spectrum of wind-generated waves. *J. Fluid Mech.*, **4**, 426–433.

— 1985: Spectral and statistical properties of the equilibrium range in wind-generated gravity waves. *J. Fluid Mech.*, **156**, 505–531.

Polnikov, V. G. and V. Inocentini, 2008: Comparative study of performance of wind wave model: Wavewatch?modified by new source function. *Engineering Applications of Computational Fluid Mechanics*, **2**, 466–481.

Ruessink, B. G., D. J. R. Walstra, and H. N. Southgate, 2003: Calibration and verification of a parametric wave model on barred beaches. *Coastal Eng.*, **48**, 139–149.

Stansell, P. and C. MacFarlane, 2002: Experimental investigation of wave breaking criteria based on wave phase speeds. *J. Phys. Oceanogr.*, **32**, 1269–1283.
`http://ams.allenpress.com/archive/1520-0485/32/5/pdf/i1520-0485-32-5-1269.pdf`

Tolman, H. L., 1992: Effects of numerics on the physics in a third-generation wind-wave model. *J. Phys. Oceanogr.*, **22**, 1095–1111.

— 2002: User manual and system documentation of WAVEWATCH-III version 2.22. Technical Report 222, NOAA/NWS/NCEP/MMAB.

Tolman, H. L. and D. Chalikov, 1996: Source terms in a third-generation wind wave model. *J. Phys. Oceanogr.*, **26**, 2497–2518.

van der Westhuysen, A. J., M. Zijlema, and J. A. Battjes, 2007: Saturation-based whitecapping dissipation in SWAN for deep and shallow water. *Coastal Eng.*, **54**, 151–170.

Vandemark, D., B. Chapron, J. Sun, G. H. Crescenti, and H. C. Graber, 2004: Ocean wave slope observations using radar backscatter and laser altimeters. *J. Phys. Oceanogr.*, **34**, 2825–2842.

Violante-Carvalho, N., F. J. Ocampo-Torres, and I. S. Robinson, 2004: Buoy observations of the influence of swell on wind waves in the open ocean. *Appl. Ocean Res.*, **26**, 49–60.

WISE Group, 2007: Wave modelling - the state of the art. *Progress in Oceanography*, **75**, doi:\bibinfo{doi}{10.1016/j.pocean.2007.05.005}, 603–674.

Wu, C. H. and H. M. Nepf, 2002: Breaking criteria and energy losses for three-dimensional wave breaking. *J. Geophys. Res.*, **107**, doi:\bibinfo{doi}{10.1029/2001JC001077}, 3177.

Young, I. R. and A. V. Babanin, 2006: Spectral distribution of energy dissipation of wind-generated waves due to dominant wave breaking. *J. Phys. Oceanogr.*, **36**, 376–394.

Fabrice's Draft: March 6, 2009

Generated with ametsocjmk.cls.

Written by J. M. Klymak

mailto:jklymak@ucsd.edu

http://opg1.ucsd.edu/ jklymak/WorkTools.html